Available online at www.sciencedirect.com
ScienceDirect
Journal of Theoretical Biology 246 (2007) 366–376
Journal of Theoretical Biology
www.elsevier.com/locate/yjtbi

An index to measure the effects of temperature change on trophic interactions

J. David Logan[a,*], William Wolesensky[b]

[a]Department of Mathematics, University of Nebraska, Lincoln, NE 68588, USA
[b]Program in Mathematics, College of Saint Mary, Omaha, NE 68134, USA

Received 18 August 2006; received in revised form 13 November 2006; accepted 30 November 2006
Available online 15 December 2006

Abstract

Experimental studies document the fact that environmental temperature changes can affect the timing of interactions in many consumer-resource systems through altered, or shifted, phenologies of the species involved. We develop a simple mathematical model that shows one method to measure, quantitatively, the magnitude of the shift. Under different temperature regimes we compute the intersection of two regions in a joint phenology space: the region where temporal interactions can occur and the region where particular-sized predators consume particular-sized prey. The area of the intersection provides a numerical value for measuring the effective interaction. A comparison of the areas for different temperature histories defines an index, or yardstick, for quantitatively assessing the effects of temperature variations on phenological shifts.

Keywords: Global temperature change; Phenology; Trophic interations

1. Introduction

It is well documented through many experimental studies that global climate change can impact species interactions at various trophic levels (e.g., Kareiva et al., 1993; Harrington et al., 1999; Burns, 2000; Walther et al., 2002; Joern et al., 2005; Visser and Both, 2005). In particular, changes in temperature can alter many consumer-resource interactions by shifting the species' phenologies and thus the temporal association, or timing, of predation events. A simple situation where timing can be altered is in the relationship between plant budburst and the need for hatched, herbivorous insects to feed; as an example, higher temperatures can accelerate the development rate of psyllids more significantly than for catkins, which turns out to favor survivorship of psyllids in warmer environments (Hill and Hodkinson, 1992). Many other ecological systems involving birds (avian migration timing, the timing of breeding), aquatic life (spawning times vs. phytoplankton blooms), and predacious and herbivorous insects involve possible timing mismatches caused by phenology shifts. The ecological literature abounds with such examples, too numerous to cite. The review by Visser and Both (2005) mentions many such systems and argues for development of a yardstick to measure phenological changes and urges researchers to share databases for analysis.

Timing events may also be decoupled by carbon dioxide levels and other environmental factors (Bazzaz, 1990); further, spatial associations can be altered as well. But, in this communication, we focus only on temperature effects.

One of the key questions in ecology is to determine how changes in synchronization affect population dynamics (Harrington et al., 1999). Our goal is to present a simple way to quantitatively assess the possible effects of temperature change on two interacting species. The calculation is based on determining the area of a region in a physiological space (joint phenology space of the two species) where interactions can occur. If the areas are calculated under different temperature regimes, their differences provide a measure, or index, of how shifts in phenologies change the interactions. The calculation is

*Corresponding author. Tel.: +1 402 472 7260; fax: +1 402 472 8466.
E-mail addresses: dlogan@math.unl.edu (J.D. Logan), wwolesensky@csm.edu (W. Wolesensky).

0022-5193/$ - see front matter © 2006 Elsevier Ltd. All rights reserved.
doi:10.1016/j.jtbi.2006.11.014

based upon the assumption that development rates for one, or both, species, measured in degree-days per day, are a known function of temperature. Such rates have been measured for a large number of exothermic taxa. The input into the computation is the time-dependent temperature history during the development period. We emphasize that population levels, or abundances, are not computed; rather we measure the development regions of both species where interactions are possible.

There have been several papers that quantitatively address ecological and phenological issues with regard to temperature effects. Relevant to the present work, the authors and colleagues (Logan et al., 2006; Joern et al., 2006; Logan et al., 2007; Wolesensky and Logan, 2007) have studied temperature-dependent, wolf spider–grasshopper interactions in grassland ecosystems, and Logan and Wolesensky (in press) have studied a model snake–vole system; all of these works involve discrete-time models based upon a temperature-dependent, predator functional response that modifies the search time for the predator. Logan et al. (1976) and Wollkind and Logan (1978)[1] have examined McDaniel spider mite-predacious spider mite interactions on apple tree foliage, and Logan and Powell (2001) have studied the temperature-dependent phenology (oviposition and developmental milestones) of mountain pine beetles to evaluate seasonality in lodgepole pine ecosystems (see also, Bentz et al., 1991; Logan and Bentz, 1999; Powell et al., 2000). Other studies include: Mack and Smilowitz (1982), Xia et al. (1999) in aphid–ladybeetle systems, Wermelinger and Seifert (1999) in spruce bark beetles, Rochat and Gutierrez (2001) in olive scale, Neuman (2003) in aphid systems, and Gilioli et al. (2005) in predacious flies and fruit flies. These references, collectively, contain a large bibliography on temperature-dependent interactions in various ecological settings and provide a gateway to the extensive literature.

2. Temperature-driven phenologies

This brief section reviews some elementary quantitative ideas regarding temperature and development (phenology).

Several physiological quantities have been used to measure an animal's or plant's development from birth to maturity (for example, age, a characteristic length, weight or other physiological attributes). Another common measurement for development, which is used in this paper, is degree-days. The idea is that a species must accumulate a certain number of days where the temperature is above some minimal threshold level. To be more specific, we consider a single, poikilothermic (or exothermic), animal species (e.g., an insect) and let ξ denote its development, measured in degree-days, over a nymphal period from emergence (at birth, at hatching or termination of diapause) to maturity. We normalize ξ so that $0 \leqslant \xi \leqslant 1$, with $\xi = 0$ at birth and $\xi = 1$ at full development. The time period over which development occurs is the nymphal period T. Thus, ξ measures phenology. To understand how ξ evolves over the nymphal period, we denote the *body* temperature of the species by $\theta = \theta(t)$, where t is continuous time measured in days, and body temperature is measured in degree Celsius. We denote the development rate by $r = r(\theta)$, given in degree-days per day. The net gain $\mathrm{d}\xi$ in degree days over a small period from t to $t + \mathrm{d}t$ is approximately $r(\theta(t))\mathrm{d}t$. Therefore, by definition, the developmental dynamics is given by

$$\frac{\mathrm{d}\xi}{\mathrm{d}t} = r(\theta(t)), \quad \tau < t < \tau + T, \tag{1}$$

with $\xi(t;\tau) = 0$ at time $t = \tau$, where τ is the time of emergence. Thus, the parameter τ is the time a single cohort appears. The nymphal period T depends upon both τ and the rate r, which, for simplicity, is not indicated in the notation; by definition, $\xi(\tau + T;\tau) = 1$. Further, we assume that both r and θ are smooth functions of their arguments, and $r \geqslant 0$. The solution to the differential equation (1) with the given initial condition is a smooth curve

$$\xi = \xi(t;\tau), \quad \tau \leqslant t \leqslant \tau + T,$$

in the $t\xi$ plane. This curve (Fig. 1) represents an individual's (or cohort's) path in physiological space-time ($t\xi$ space), and it can be calculated via direct integration of (1) to get

$$\xi(t;\tau) = \int_{\tau}^{t} r(\theta(s))\,\mathrm{d}s. \tag{2}$$

In the graphical representation in Fig. 1 of physiological space-time we have put t and ξ on the horizontal and vertical axes, respectively; this is the opposite of a common representation used in applied mathematics and partial differential equations where time is on the vertical axis (e.g., see Logan, 2006). In the context of advection equations, this path is a characteristic curve. In the present discussion we shall refer to $\xi = \xi(t;\tau)$ as a *cohort curve*, and it is the locus of points in physiological space-time along which development occurs. The nymphal period T is determined by the condition

$$1 = \int_{\tau}^{\tau+T} r(\theta(s))\,\mathrm{d}s. \tag{3}$$

In summary, if the temperature history and development rate are known, then the species' cumulative development can be calculated by (2). If all the cohorts emerge between times τ and σ, with $\sigma > \tau$, then the domain of physiological space-time where the cohorts exist is the region between the two cohort curves $\xi = \xi(t;\tau)$ and $\xi = \xi(t;\sigma)$. See Fig. 1. Because different cohorts experience the same temperature at the same time, different cohort curves are shifted vertically from each other when there is a common domain; thus, the speeds of the cohort curves (or rate of development) along the same vertical line are the same. Further,

[1]There are citations to both J. David Logan (author) and to Jesse A. Logan in this paper.

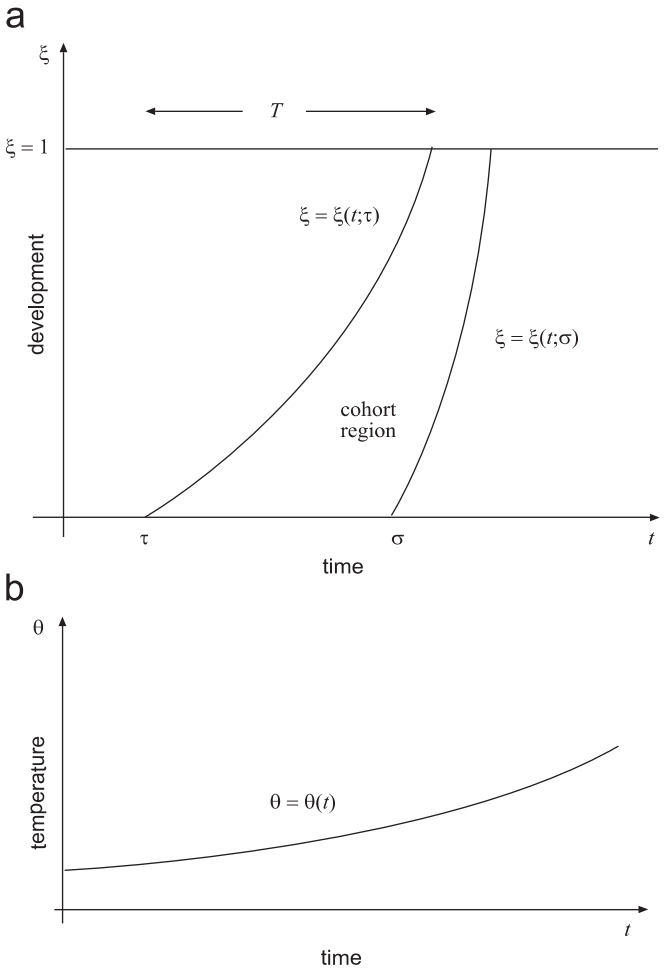

Fig. 1. (a) Two cohort development curves $\xi = \xi(t;\tau)$ and $\xi = \xi(t;\sigma)$ in development-time (ξt) space for cohorts emerging at times τ and σ. The cohort region represents development-time values of all cohorts emerging between times $t = \tau$ and $t = \sigma$. The time T is the development period of the cohort hatching at time τ. (b) The temperature history $\theta = \theta(t)$ represents an increasing body temperature over a season. The speeds (slope) of the cohort curves in (a) increase with increasing temperature.

we are assuming no natural variability in a cohort as it evolves through its development period.

We observe also that the preceding discussion applies to passage through a single development stage, e.g., an instar, where $\xi = 0$ and 1 represent the emergence of that instar and the completion of that instar, respectively.

Another caveat should be mentioned. First, the body temperature is usually not equal to the ambient air temperature. Most poikilothermic animals thermoregulate via behavior to maintain body temperatures within a certain range (for example, by orienting their body to solar rays, or by seeking shade in the environment), and therefore body temperature is more closely related to the local environmental or micro-habitat temperature than to air temperature. Complicated relations may exist between the ambient air temperature and habitat temperature (e.g., see Lactin and Johnson, 1998; Logan et al., 2006 for a study with grasshoppers) depending upon the solar radiation (cloudy vs. sunny) and the complexity of the forage and environment. For simplicity, these temperature complications are not included in the present model. When we use the word temperature, we will mean *average* body temperature θ. Our assumption about the body temperature is that $\theta(t)$ is a given function of time over a season representing the *average* daily body temperature of the animal or plant on day t. In specific examples we take $\theta(t)$ to be a linear or quadratic function. Such approximations are reasonable because many animals thermoregulate to quickly bring their body temperature up to an optimal level. As the ambient air temperature increases through the summer, for example, the animal will have a larger portion of the day near its optimum temperature, so the average body temperature will increase as well.

The development rate $r = r(\theta)$ is often taken as a linear function of temperature, giving a Q_{10} type rule (the rate doubles every 10° increase in temperature). But, in fact, development rates of most poikilothermic animals and many plants are strongly nonlinear functions of temperature, as shown in Fig. 2. There is an optimal temperature θ_{opt} where the development rate is maximal, and below a certain threshold temperature θ_{min} the development rate is zero. Beyond the optimum temperature there is a rapid fall-off with increasing risk of death. The common, linear response is an approximation for a limited range of temperatures (see Fig. 2). Development rates have been measured for many species, both plant and animal, and the data are often fit to a regression curve with specific formula (Li and Jackson, 1996 for spiders and grasshoppers; Shenk, 1996 for trees; Lactin and Johnson, 1998; Hilbert and Logan, 1983). A theoretical, kinetic basis for such rates is discussed in Gillooly et al. (2002) and the references therein.

In principle, Eq. (2) can always be solved numerically to obtain the cohort dynamics. In special cases, the cohort curves can be determined analytically.

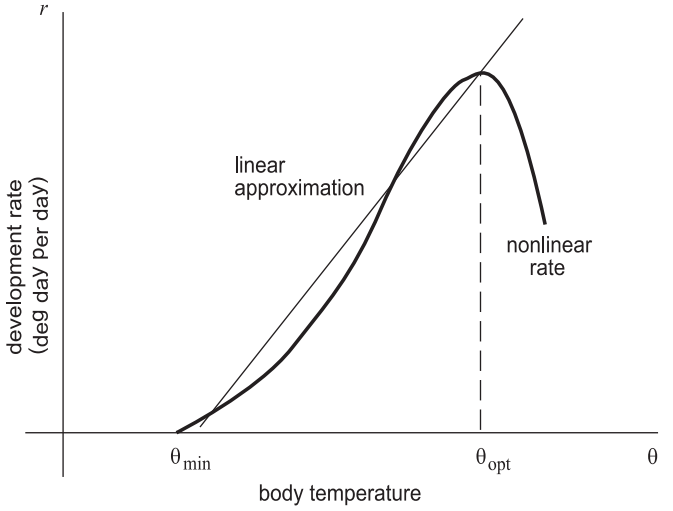

Fig. 2. Schematic of a generic, nonlinear rate function $r = r(\theta)$ and its linear approximation over a restricted range of temperatures. For illustration purposes, we exaggerated the difference between the nonlinear curve and its approximation in this range; in specific cases the approximation is highly accurate.

Again, we can interpret the cohort region in Fig. 1 in a way to accommodate development progress from any initial stage; for example, the interval $0 \leqslant \xi \leqslant 1$ could represent the development of an insect through its third instar.

Example 1. If the development rate is independent of temperature, i.e., $r = r_0$, then the cohort curves are parallel straight lines of the form $\xi = r_0(t - \tau)$, regardless of the temperature profile. However, the hatching date for these species may change under temperature variations because there is no thermoregulation in the pre-emergence, or egg stage. Thus, warmer temperatures, for example, can induce an earlier hatching date, or colder temperatures can delay hatching.

Example 2. Consider the special case when the temperature and the development rate are linear functions; that is,

$$r = \alpha\theta - \beta, \quad \theta = \gamma t + \theta_0,$$

where $\beta/\alpha \leqslant \theta \leqslant \theta^*$, where θ^* is the temperature at maximum development rate, and $\theta_0 \geqslant \beta/\alpha$. This is the case when the temperature increases linearly during the relevant time period and is in the range where the development rate can be approximated by a linear (e.g., a Q_{10}) type rule. Then $r(\theta(t)) = \alpha\gamma t + \alpha\theta_0 - \beta = at + b$, where $a = \alpha\gamma$ and $b = \alpha\theta_0 - \beta$, and the cohort paths (2) in physiological space-time form a family of (concave up) parabolas given by

$$\xi = \frac{a}{2}(t^2 - \tau^2) + b(t - \tau), \tag{4}$$

where τ is the time the cohort emerges. The nymphal period T for cohort τ is determined first by solving the quadratic equation $(a/2)(t^2 - \tau^2) + b(t - \tau) = 1$, which gives the time that development is complete:

$$t^* = \frac{1}{a}\left(-b + \sqrt{b^2 + 2a\left(\frac{a}{2}\tau^2 + b\tau + 1\right)}\right).$$

Then $T = t^* - \tau$. For a numerical illustration, corresponding for example to a cohort of grasshoppers, we take $r = 0.002\theta - 0.03$, $\theta = 0.15t - 2.5$, $150 \leqslant t \leqslant 250$, where time is measured in Julian days. This rate gives a 25-day nymphal period at the constant maximum temperature of 35° corresponding to a maximum rate of 0.04 deg-day per day. The average body temperature is a linear approximation varying from 20° on Julian day 150 to 35° on Julian day 250. The parameters a and b are given by $a = 0.0003$, $b = -0.035$. For a cohort hatching on the 150th day, this corresponds to a nymphal period of approximately of 55 days (Eq. (3)). For a cohort hatching 15 days later, on the 165th day, the nymphal period is 47 days.

These examples are generic cases where analytic formulas can be obtained. But, in principle, cohort curves can be obtained for any nonlinear development rate and any temperature history by numerical integration. Further, relations between body temperature and ambient air temperature can be included as well. The concepts apply to both plant and animal species.

3. Interacting species

Based on considerations in the preceding section applied to two different species, we now develop and introduce a numerical index of the interaction that measures the shifts of phenologies under different temperature profiles. The two species represent a resource and a consumer, e.g., prey and predators, or plants and insect herbivores. To fix the idea we consider prey and predators. We assume the developmental dynamics of the prey is given by (1), and we consider a second trophic level, the predator, with development rate $\rho = \rho(\theta)$. If η represents the normalized development variable for the predator, then

$$\frac{d\eta}{dt} = \rho(\theta(t)),$$

and the predator cohort emerging at time $t = \kappa$ has cohort curve given by

$$\eta = \eta(t;\kappa) = \int_\kappa^t \rho(\theta(s))\,ds,$$

with $\eta(\kappa;\kappa) = 0$ and $\eta(\kappa + T;\kappa) = 1$, where T is the development period (dependent upon κ). Predator cohorts emerging in the time interval $[\kappa, \lambda]$ will evolve in physiological space-time between the curves $\eta = \eta(t;\kappa)$ and $\eta = \eta(t;\lambda)$, in $0 \leqslant \eta \leqslant 1$. A figure can be drawn similar to Fig. 1.

An obvious, yet key, observation is that both species must be present at the same time for predation to occur. This temporal constraint defines a planar region in $\xi\eta$ space (joint phenology space) where interactions can occur. To see this graphically we construct on a single set of axes (development vs. time) the regions in physiological space-time of two cohorts (prey hatching in $\tau \leqslant t \leqslant \sigma$ and predators emerging in $\kappa \leqslant t \leqslant \lambda$). In Fig. 3, for illustration purposes, we have drawn the cohort curves as straight lines. The set S of relevant times are those times for which both predators and prey are present. In Fig. 3 this is the time of emergence of the first prey to the time of the final prey cohort to mature. For any fixed time t in the set S, represented by a vertical line in Fig. 3, we can plot in the $\xi\eta$ plane the domain D_t where both species exist at the same time. This domain D_t, being the Cartesian product of two intervals (the interval of development space where the prey exists and the interval where the predator exists), is a rectangle, possibly a degenerate one (a point or a line). For example, three such times are shown in Fig. 3, the times t_1, t_2, t_3. To each corresponds a rectangle D_{t_i}, $i = 1, 2, 3$ (illustrated in Fig. 4). To illustrate how D_{t_1} is obtained, for example, we note (Fig. 3) at time t_1 predators exist with development $0 \leqslant \eta \leqslant a$ and prey exist with development $0 \leqslant \xi \leqslant b$; thus $D_{t_1} = [0, b] \times [0, a]$, as shown in Fig. 4. The regions D_{t_2} and D_{t_3} are computed similarly. All possible phenological-time interactions between the two species are

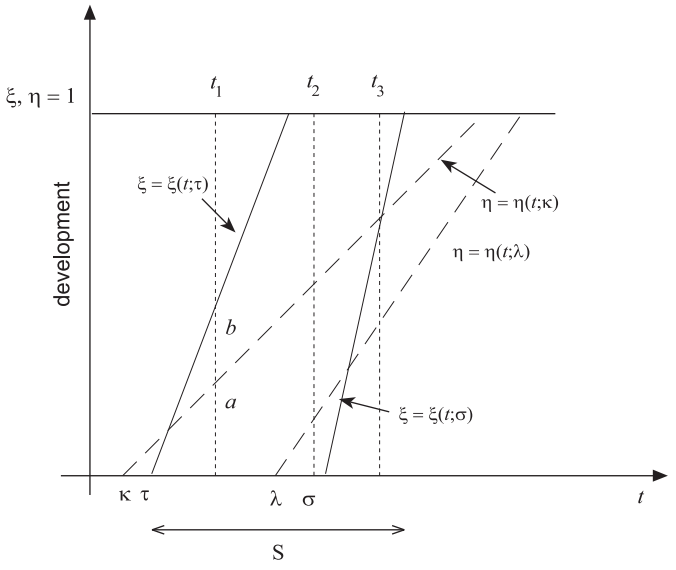

Fig. 3. Schematic of a development-time diagram indicating an interaction of a cohort of prey (between the solid oblique lines) emerging in the time interval $\tau \leqslant t \leqslant \sigma$ with a cohort of predators (between the dashed oblique lines) emerging in the interval $\kappa \leqslant t \leqslant \lambda$. The time interval S consists of those times when both prey and predators are present. We have indicated three fixed times (dotted vertical lines) t_1, t_2, and t_3 in S at which the rectangles D_{t_1}, D_{t_2}, and D_{t_3} are determined (see Fig. 4).

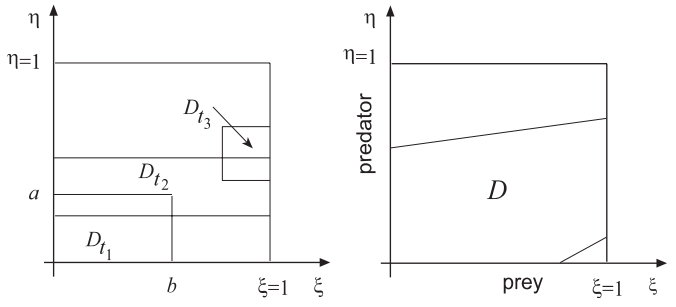

Fig. 4. For illustration, the plot on the left shows three rectangles D_{t_1}, D_{t_2}, and D_{t_3} corresponding to the times t_1, t_2, and t_3 in Fig. 3. For example, the rectangle D_{t_1} is the Cartesian product of the intervals $0 \leqslant \xi \leqslant b$ and $0 \leqslant \eta \leqslant a$, and it is the set of development stages of predators and prey that are present at time t_1. The region $D = \bigcup_{t \in S} D_t$ is the union (sum) of all the rectangles D_t as t varies over the set of times S that both predators and prey are present. It represents the region in phenology space of possible temporal interactions between the two species. Note that the small region in the lower right corner is excluded from D because at all times very small predators are not present when very large prey are present.

therefore the sum (union) of all the domains D_t as t ranges over the times in the set S where both exist simultaneously. We call this domain D. Fig. 4 indicates this region for the interaction shown in Fig. 3. Thus,

$$D = \bigcup_{t \in S} D_t.$$

To elaborate, D is the subset in the two-dimensional $\xi\eta$ space of predator–prey phenologies where they can interact in the time period under consideration. We refer to D as the *region of temporal interactions*. The area of D measures the level of possible interactions in time. When the temperature history changes, the phenologies will be altered; hence, the cohort regions will shift and the region D will change to a different region D'. One way to estimate how much temperature change will affect temporal phenology interactions is to compare the areas of D and D' (e.g., by measuring the percentage change).

However, it is often the case that only certain sized predators will consume certain sized prey items. For example, small predators in early stages of development may not consume large prey. Here, we are implicitly assuming a relationship between size and development. Thus, there is a region E of $\xi\eta$ space defined by the set of (ξ, η) for which a predator of size η can consume a prey item of size ξ. We refer to E as the *region of physical interaction*. (In models for interactions between grasshoppers and wolf spiders, for example, this region is bounded below by a positively sloped straight line, Joern et al., 2006; see also Turner, 1979.) The *effective domain of phenological interaction* is the intersection $D \cap E$ of the domain D and the domain E (Fig. 5). The portion of the region E of physical interaction where predation can occur over the relevant time period, that is, the ratio of the area of the intersection $D \cap E$ to the area of E, is a numerical value

$$\frac{\text{Area}(D \cap E)}{\text{Area}(E)}. \tag{5}$$

This ratio can be used to define phenology shifts in the following manner. Under a change in the temperature history, the region of effective phenological interaction changes from $D \cap E$ to $D' \cap E$, and we can compute the ratio (5) for each region. Then we define the *phenology shift index* (PSI) by

$$\text{PSI} = \frac{\text{Area}(D' \cap E)}{\text{Area}(E)} \div \frac{\text{Area}(D \cap E)}{\text{Area}(E)} = \frac{\text{Area}(D' \cap E)}{\text{Area}(D \cap E)}. \tag{6}$$

Computing the PSI for different temperature regimes provides a simple numerical index, or yardstick, that

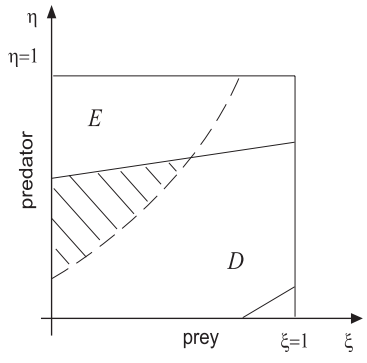

Fig. 5. For the generic case, the regions D and E in phenology space and their intersection (shaded) $D \cap E$, which is the effective domain of interaction. The region E is the region of physical interaction representing the set of all (ξ, η) for which a predator in stage η can consume a prey item in stage ξ. A numerical measure of the interaction is the ratio $\text{Area}(D \cap E)/\text{Area}(E)$, which represents the portion of possible physical interactions that can occur over the given time period S.

indicates the change in interaction due to phenology shifts. (One could equally well define PSI to be the relative, or percentage, change.)

There is one noted aspect to the calculation of the PSI. Although it seems straightforward, computing the areas of the regions D and $D \cap E$ involve a nontrivial numerical calculation. We performed this calculation in MATLAB and a copy of the program (m-file) can be obtained from the authors.

We now illustrate this theory (in Example 3) with a numerical calculation where both predator and prey are subject to development periods, and there are shifts in phenologies caused by temperature changes. Following Example 3 we explain, in Section 4, how the theory can be adapted to the special case where one of the species, either the predator or the prey, does not undergo a development period.

Example 3. As remarked by Visser and Both (2005), there is a lack of good, specific, long term data sets on phenologies that can be linked to theoretical studies on the impacts of global climate change. The generic example we consider below was initially motivated by studies of grasshopper populations in midwest, grassland ecosystems, and in part by the studies of Joern et al. (2006) related to the control of grasshoppers by wandering wolf spiders (lycosa). However, in these experiments it was found that the spider distribution, in both number and size, was more or less uniform throughout the grasshopper nymphal period, giving no evidence in rangeland systems that the spider's phenology is offset in such a way as to reduce possible interactions. (It was shown, on the other hand, that temperatures do affect hourly activity periods, and hence the spider's functional response, during the day; see Logan et al., 2006.) Generally, the spider–grasshopper interaction is greatly complicated by vegetation structure, micro-habitat temperature, and both grasshopper and spider thermoregulation, and therefore the interaction does not provide the data set needed for a detailed example.

Nevertheless, the phenology shifts of grasshoppers provide good order-of-magnitude values and quantities to theoretically study effects of climate change with respect to other predators. They exhibit tremendous variation in development depending upon temperature, geographic location and species (Joern and Gaines, 1990). Grasshopper predators, other than spiders, include birds, predacious insects (e.g., robber flies, which are discussed in Section 4), parasitoids, and a variety of fungi and other pathogens. For this example we consider a generic predator with a constant development rate having a 25-day development period, independent of temperature. Thus, the predator's development rate is $\rho = 0.04$ deg-day/day.

For the grasshopper cohort we assume quantities characteristic of a species in warmer climates. We will take the average daily temperature to be in the range where the development rate can be approximated by a linear function of body temperature (see Fig. 2),

$$r = \alpha\theta - \beta. \tag{7}$$

We take $\alpha = 0.045$ and $\beta = 0.09$. Then, at 35° the prey will mature in 14.8 days, while at 30° it will mature in 22.2 days. We stipulate that there is no development below $\theta = 20°$, the threshold temperature. These parameter values are characteristic of values for *M. sanguinipes* (Hilbert and Logan, 1983) reared in a laboratory in the range of higher temperatures. The average body temperature of the prey is assumed to be a concave-down, quadratic function

$$\theta(t) = \gamma + 0.25(t - t_0) - 0.002(t - t_0)^2, \tag{8}$$

where γ is the body temperature on Julian day t_0. For the baseline calculation we take $\gamma = 27$ on day $t_0 = 120$ (May 1). In this case $r(\theta(t))$ is a quadratic function, and so a prey cohort curve $\xi = \xi(t;\tau)$ is a cubic function. Integration gives cohort curves

$$\xi(t;\tau) = (\alpha\gamma - \beta)(t - \tau) + \alpha\{0.125((t - t_0)^2 - (\tau - t_0)^2) - 0.001((t - t_0)^3 - (\tau - t_0)^3)\},$$

where τ is the day of emergence. The nymphal period can be determined numerically by solving $\xi(t;\tau) = 1$ for t. The predator cohort curves form a family of straight lines $\eta = 0.04(t - \kappa)$, where κ is the emergence day. We assume that the region E of physical interactions is the region $\eta \geqslant 0.5 + 0.25\xi^2$ bounded below by the convex quadratic function $\eta = 0.5 + 0.25\xi^2$ (shaded region in Fig. 6). Thus, relating phenology to size, larger predators consume prey of most sizes.

Fig. 7 displays the results for a baseline calculation. Fig. 7a shows the two species' cohort regions and their overlap. The solid (cubic) curves bound the prey cohort region, and the dashed (linear) curves bound the predator cohort region. Both prey and predator first emerge on Julian day 132, and the final emergence day is Julian day 142 for both. Fig. 7b shows the region D of possible temporal interactions, and finally, Fig. 7c shows the effective region of interaction, i.e., the intersection of regions D and E (region E is shown in Fig. 6); its area is

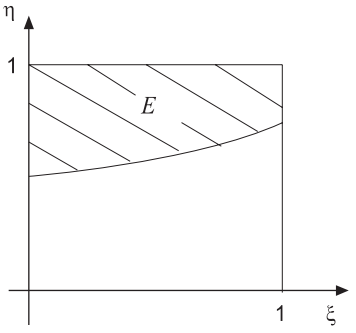

Fig. 6. In Example 3, the region $E : \eta \geqslant 0.5 + 25\xi^2$, $0 \leqslant \xi \leqslant 1$, in development space where possible interactions, or predation events, between the two species can occur. This region applies to calculations shown in 8–10. The interpretation is that larger predators consume prey of mostly all sizes.

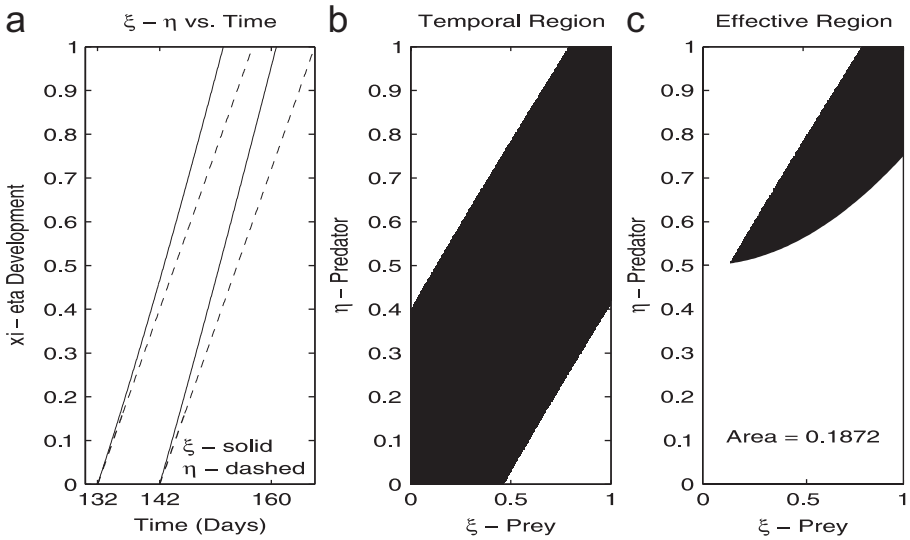

Fig. 7. These plots show the baseline calculation. Both predator and prey emerge between Julian day 132 and 142. The average prey body temperature is given by (8). Subplot (a) shows the prey and predator cohort regions in development-time space. Subplot (b) gives the corresponding region D of temporal interaction in $\xi\eta$ phenology space. Subplot (c) shows the effective region of interaction, $D \cap E$, and its area. The region E is shown in Fig. 6.

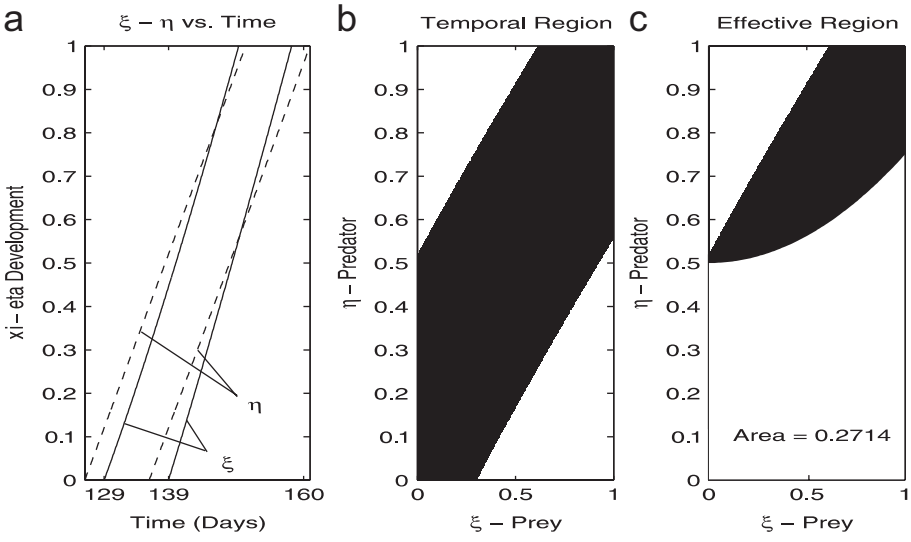

Fig. 8. These plots show the calculation when the temperature is increased so that the prey emerge 3 days earlier, between Julian day 129 and 139, and the predator emerges 6 days earlier, between Julian day 126 to 136. Subplot (a) shows the prey and predator cohort regions in development-time space. Subplot (b) gives the corresponding region D' of temporal interaction in $\xi\eta$ phenology space. Subplot (c) shows the effective region of interaction, $D' \cap E$, and its area. The region E is shown in Fig. 6.

given by $\text{Area}(D \cap E) = 0.1872$. Reiterating, this area is a quantitative measure of the effective phenological interaction, and it combines both the possible temporal interactions and the physical interaction.

Now we determine the effect of a temperature increase that causes both prey and predator emerge at earlier dates—the prey 3 days earlier and the predator 6 days earlier from that in Fig. 7. Fig. 8a shows the cohort regions with Julian emergence days 129–139 for the prey, and 126–136 for the predator. Compared to the baseline in Fig. 7a, the temporal overlap is larger. Fig. 8b, which shows the region D' associated with Fig. 8a, confirms the larger temporal interaction. Fig. 8c shows the effective region $D' \cap E$ of interaction with $\text{Area}(D' \cap E) = 0.2714$. Therefore, the PSI for the temperature increase is

$$\text{PSI} = \frac{\text{Area}(D' \cap E)}{\text{Area}(D \cap E)} = \frac{0.2714}{0.1872} = 1.449.$$

This means there is about a 45% increase in the effective region of interaction when the temperature increases. We therefore expect more predation with a negative effect on the prey and a positive effect on the predator.

Next we change the temperature history to a lower average temperature, causing the prey to emerge later,

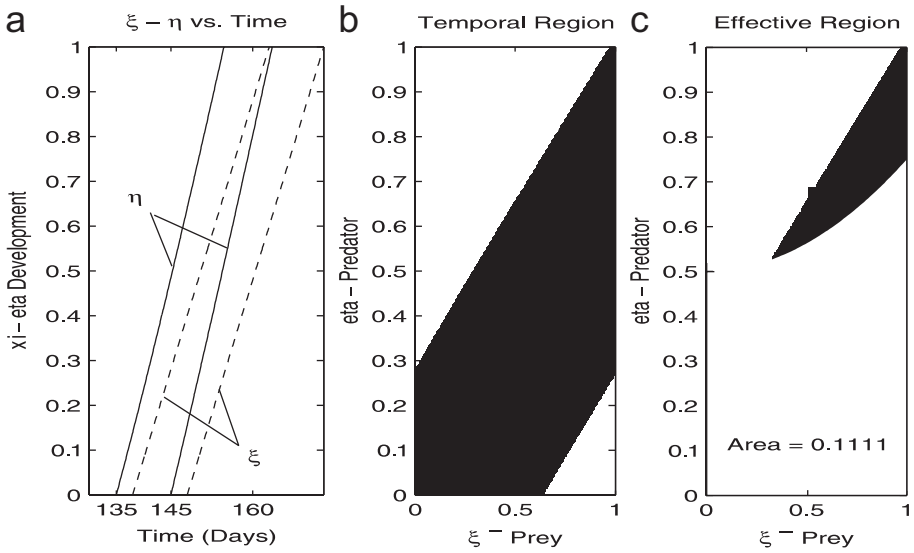

Fig. 9. These plots show the calculation when the temperature is decreased so that the prey emerge later than baseline, between 135 and 145 days, and the predator emerges between Julian day 138 and 148. Subplot (a) shows the prey and predator cohort regions in development-time space, and subplot (b) gives the corresponding region D'' of temporal interaction in $\xi\eta$ phenology space. Subplot (c) shows the effective region of interaction, $D'' \cap E$, and its area. The region E is shown in Fig. 6.

during the Julian day period 135–145 days, and the predator to emerge between 138 and 148 days. Fig. 9a shows the overlap domain, which is considerably reduced when compared to the baseline in Fig. 7a. Fig. 9b shows the region D'' corresponding to Fig. 9a, and the effective region of interaction $D'' \cap E$ is plotted in Fig. 9c; it has area given by $\text{Area}(D' \cap E) = 0.111$. The PSI index for the temperature decrease, when compared to the baseline, is

$$\text{PSI} = \frac{\text{Area}(D'' \cap E)}{\text{Area}(D \cap E)} = \frac{0.111}{0.1872} = 0.593.$$

Therefore, under cooler temperatures there is about a 40% reduction in the effective interaction. In this case we might expect predation to decrease, giving a negative effect on the predator and a positive effect on the prey.

In general, one cannot predict, in advance, whether the change in interaction will increase or decrease under a temperature change, or under later or earlier emergence of a predator. The direction of the change is highly dependent upon the region E of physical interaction and the speeds of development. The preceding analysis leads to the correct conclusion and gives a quantitative estimate of the magnitude.

4. Special cases

There are many examples of trophic interactions where one of the species is not in a development process, but rather in an adult stage or some other fixed stage. In this section we show how these interactions fit into the general framework discussed in the previous sections.

An example is bud burst, where a developing herbivorous insect feeds on young, tender plant materials, such as buds on a tree. The buds appear during a fixed time interval and can be considered prey items for as long as they exist; we do not consider them passing through a development stage. Another example is an adult insect that, upon emerging from its pupal stage, becomes a predator of certain instars of another insect passing through its development stages. Specific cases of these two phenomena are winter moth larvae feeding on oak buds and adult robber flies feeding upon the later instars of grasshoppers.

We first discuss oak bud burst and winter moth larvae. In the ideal case where interactions are synchronous, the moth eggs hatch during the bud burst period, and the larvae have young plant material on which to feed. But, under temperature change, the timing of these events can shift. Moth eggs that hatch before or after the bud burst period must feed on older plant material having a chemical composition that leads to reduced fitness of female moths (smaller females with reduced egg loads). In fact, it has been observed in the Netherlands that the bud burst has advanced, but winter moths have advanced more, leading to mistiming (see Buse and Good, 1996; Visser and Holleman, 2001; the review by Visser and Both, 2005 cites numerous studies). However, because this interaction is so complex, especially in extreme climatic conditions, there is still some conflict among ecologists whether synchrony has been disrupted.

In any case, we can study this interaction using the framework of the theory. In the following we maintain our notation, using ξ and η as the development variables for the prey and predator, respectively. We represent bud burst existence in the development time space (ηt space) of the moth as a rectangle bounded by the vertical lines $t = \tau$ to $t = \sigma$. We interpret the η axis as defining a domain where all edible material, i.e., all stages of buds, is present at the

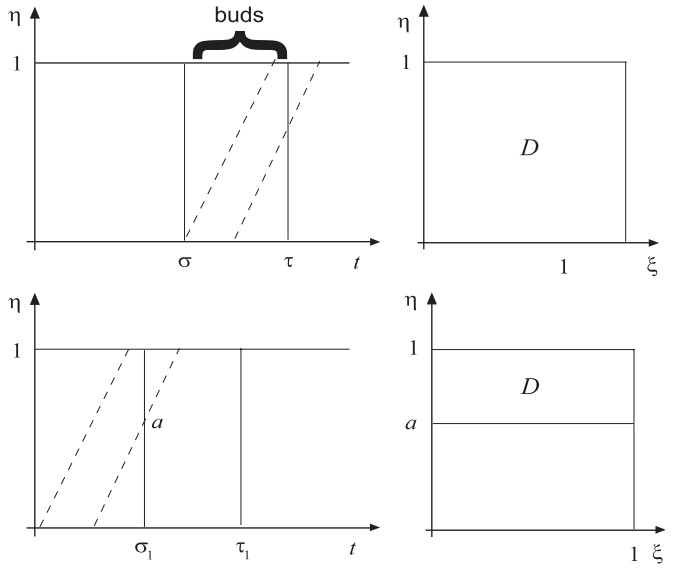

Fig. 10. Bud burst. The top two plots show a baseline situation where buds emerge between times τ and σ. A cohort of consumers, e.g., developing moth larvae, are present in the region between the dashed lines. The region D is the entire square (top right) because all buds are available at all times. It is assumed that all sized larvae consume buds, so E is the entire square, giving $D \cap E = D = E$. The lower two panels show the change when both the consumer and the resource emerge earlier, caused by higher temperatures, with the consumer shift being higher. Then $D \cap E = D$ is on the order of 60% smaller than in the baseline case, suggesting a 60% decrease in interaction.

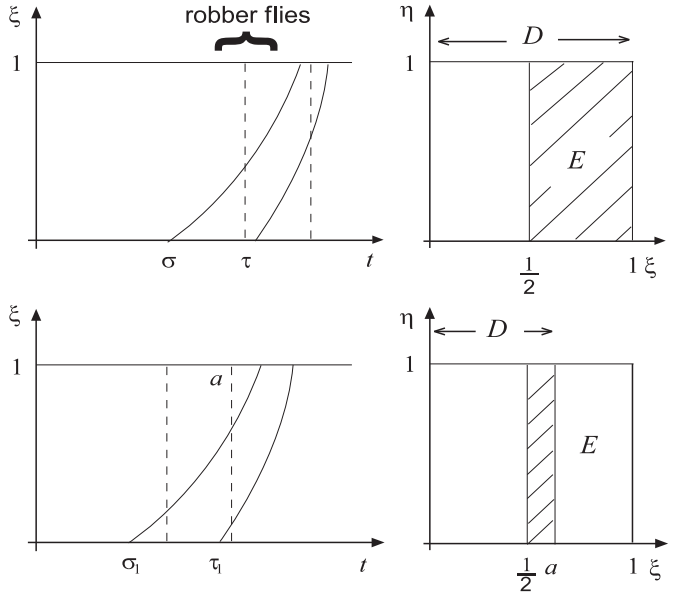

Fig. 11. Robberflies. The top left panel shows the interaction between a cohort of developing grasshoppers (solid curves) and a cohort of adult (nondeveloping) robberflies. The temporal region D is the entire square. If we assume that adult flies consume prey that have larger size, or later instars, for example, $\xi \geqslant \frac{1}{2}$, then the effective region of interaction is $D \cap E = E$ (shaded). The lower two panels show the result of an increased temperature regime where both species emerge earlier. The physical region E is the same, and D is reduced considerably, to the region $0 \leqslant \xi \leqslant a$, where a is shown. Now $D \cap E$ is approximately 25% of its baseline size, suggesting a 25% decrease in interaction.

instant of the first bud burst. The development of the moth larvae is represented by a (oblique) cohort region as defined in Section 2. For illustration we take the moth cohort curves to be straight lines. Fig. 10a represents the ideal, baseline conditions; moths hatch during the period when buds are available. Both the temporal region D and the physical region E coincide the entire square $\leqslant \xi\eta \leqslant 1$, and therefore $D \cap E = 0$ is the entire square (Fig. 10b). Under temperature increase, the bud burst zone shifts to an earlier date ($\tau_1 \leqslant t \leqslant \sigma_1$), but the cohort of moths shifts more, giving the temporal interaction shown in Fig. 10c. Now young larvae have no buds to consume. Fig. 11d shows the region of temporal interaction $D : \eta \geqslant a$, which coincides with $D \cap E$. The ratio of the areas in Figs. 10b and d defines the magnitude of the shift.

Robber flies and grasshoppers offer a similar example, with the roles of predator and prey reversed. (In the last section we discussed the phenology of grasshoppers.) Grasshoppers, the prey, develop through a sequence of nymphal instars from hatching to adult. A common predator is robber fly, a predacious fly (Diptera: asilidae) that, in its flying adult stage, attacks a variety of large insects (Joern and Rudd, 1982), including grasshoppers in certain stages (Quinn et al., 1993). Various species of these flies exist throughout North America, and, in particular, in grassland environments. Asilids are aggressive, opportunistic generalists that lay eggs in damp soil or dead wood where their larvae and pupa develop. They emerge as flying predacious insects that frequently attack larger-sized instars and adults. We model the presence of the adult robber fly population (e.g., *E. coulei*, which swarms in parts of the late spring and early summer, overlapping the developing grasshoppers; see Cannings, 1998) as a region $\kappa \leqslant t \leqslant \lambda$ in the development space $t\xi$ of the grasshopper.

The panels in Fig. 11 show a generic interaction between the two species. The cohorts of adult robber flies exist in a rectangular region of development time (ξt) space, where the development variable ξ is that of the grasshoppers. The cohort of newly hatched grasshoppers emerge between times τ and σ. We assume that the adult robber flies consume grasshoppers of size (development) $\xi \geqslant \frac{1}{2}$, which defines the region E of physical interaction. Fig. 11a shows a synchronous interaction where larger grasshoppers coexist with adult robber flies. The region D of temporal interaction is the entire square, and so the effective region is $D \cap E = E$ (shaded in Fig. 11b). Under temperature increase Fig. 11c depicts earlier emergence of both the grasshoppers and the robber flies, with the former shifting more. This leads to the mistiming of events and the region D decreases to $D : \xi \leqslant a$, as shown in Fig. 11d. Now the effective region is $D \cap E : \frac{1}{2} \leqslant \xi \leqslant a$ (shaded). Therefore, shifts in emergence time significantly reduce the interaction.

We observe that a similar situation and analysis may hold for migrating birds and grasshoppers, where the

temporal domain of the birds represents the beginning to the end of a migratory pause.

5. Summary

We defined a simple numerical index PSI that measures the level of phenology shift when temperature changes. It includes the possible temporal and physical associations between the two species in a joint phenology space. The index is the ratio (6) of the areas of the two effective domains of interaction for two temperature regimes. A value of $\mathrm{PSI}<1$ implies a potential decrease in species interactions, and a value $\mathrm{PSI}>1$ implies a potential increase in interactions. Because PSI is a quantitative measure, comparisons of the changes in interactions can be made for several different temperature histories.

In advance, one cannot always predict the direction of change in interaction—that increased interaction is always a result of earlier emergence of the predator before the prey, or decreased interaction if the predator emerges after the prey. The direction of the change depends highly upon the region D of temporal interactions and the region E where physical interactions occur (which sized predators consume which size prey). For example, if the two species are such that only small predators consume small prey, then a shift to an earlier emergence time of the predators can cause only the large predators to be present when small prey are present, and there will be a decrease in the interaction; small predators will then emerge when there are few small prey (see the robber fly example in Fig. 11). The index we define gives the precise direction of the change, and its value provides a quantitative assessment of the change, more descriptive than qualitative statements such as ''there is more interaction'', or ''there is less interaction''. One can make quantitative, numerical statements about the relative changes that occur; just for example, we could say there is a 25% decrease in interaction when the average temperature increases 5°. This shows the utility of the measure.

We illustrated the ideas with simple, generic examples. However, real ecological interactions with complicated development rates and temperature variations can be handled in the same manner; in these cases the calculations are numerical at each stage. Computing PSI for several temperature regimes can give an ecologist a numerical assessment of the possible effects of climate change on trophic interactions, and it may suggest strategies for developing appropriate data sets to study phenology changes.

While the PSI provides a quantitative measure of the potential effects of a temperature induced phenology shift, it does not predict numerical population densities of the species and their dynamics. To examine how index is related to a measurable, dynamical quantity requires the formulation and solution of a system of physiologically structured population equations (e.g., see Auslander et al., 1974; Metz and Diekmann, 1986; de Roos, 1997) in development and time variables. Because interaction at time t can occur only in the effective phenological domain $D_t \cap E$ that we introduced, the characteristic function $\chi_{D_t \cap E}$ of $D_t \cap E$ (equal to unity if (ξ, η) belongs to $D_t \cap E$, and zero otherwise) will be a multiplicative factor in the predation rate in the local balance law (partial differential equation) for prey dynamics, turning predation *on* or *off* in the development space-time region where dictated. A full discussion of such a dynamical population model is not in the scope of the present work.

Acknowledgments

The research was funded by the Biological and Environmental Research Program (BER), US Department of Energy, through the Great Plains Regional Center of NIGEC (National Institute for Global Environmental Change) under cooperative agreement No. DE-FC02-03ER63613, subcontracted through Kansas State University. The authors thank Professor Tony Joern at Kansas State University for his generous support and input on this project.

References

Auslander, D.M., Oster, G.F., Huffaker, C.B., 1974. Dynamics of interacting populations. J. Franklin Inst. 277 (5), 345–376.

Bazzaz, F.A., 1990. The response of natural ecosystems to rising global CO_2 levels. Annu. Rev. Ecol. Syst. 21, 167–196.

Bentz, B.J., Logan, J.A., Amman, G.D., 1991. Temperature dependent development of the mountain pine beetle and simulation of its phenology. Can. Entomol. 123, 1083–1094.

Burns, W., 2000. Bibliography: Climate change and its impact on species and ecosystems, www.eelink.net/~asilwildlife/CCWildlife.html.

Buse, A., Good, J.E.G., 1996. Synchronization of larval emergence in winter moth (*Operophtera brumata L.*) and budburst in pedunculate oak (*Quercus robur L.*) under simulated climate change. Ecol. Entomol. 21, 335–343.

Cannings, R.A., 1998. Robber flies (Insecta: Diptera: Asilidae). In: Smith, I.M., Scudder, G.G.E. (Eds.), Assessment of species diversity in the Montane Cordillera Ecozone. Ecological Monitoring and Assessment Network, Burlington.

Gilioli, G., Baumgartner, J., Vacante, V., 2005. Temperature influences on functional response of *Coenosia attenuata* (Diptera: Muscidae) individuals. J. Econ. Entomol. 98 (5), 1524–1530.

Gillooly, J.F., Charnov, E.L., West, G.B., Savage, V.M., Brown, J.M., 2002. Effects of size and temperature on development time. Nature 17, 70–73.

Harrington, R., Woiwod, I., Sparks, T., 1999. Cimate change and trophic interactions. Trends in Evol. and Ecol. 14, 146–150.

Hilbert, D.W., Logan, J.A., 1983. Empirical model of nymphal development for the migratory grasshopper *M. sanguinipes* (Orthoptera: Acrididae). Environ. Entomol. 12, 1–5.

Hill, J.K., Hodkinson, I.D., 1992. Effect of temperature on phenological synchrony and altitudinal distribution of jumping plant lice (Hemiptera: Psylloidea) on dwarf willow (*Salix lapponum*) in Norway. Ecol. Entomol. 20, 237–244.

Joern, A., Rudd, N.T., 1982. Impact of predation by the robber fly Proctacanthus milbertii (Diptera: asilidae) on grasshoppers (Orthoptera: acrididae) populations. Oecologia 55 (1), 42–46.

Joern, A., Gaines, S.B., 1990. Population Dynamics and Regulation in Grasshoppers. In: Chapman, R.F., Joern, A. (Eds.), Biology of Grasshoppers. Wiley, New York, pp. 415–482 (Chapter 14).

Joern, A., Logan, J.D., Wolesensky, W., 2005. Effects of global climate change on agricultural pests: possible impacts and dynamics at population, species interaction, and community levels. In: Lal, R., Stewart, B.A., Uphoff, N., Hansen, D.O. (Eds.), Climate Change and Global Food Security. CRC Press, Boca Raton, pp. 321–362 (Chapter 13).

Joern, A., Danner, B.J., Logan, J.D., Wolesensky, W., 2006. Natural history of mass-action in predator-prey models: A case study from wolf spiders and grasshoppers. The American Midland Naturalist 156, 52–64.

Kareiva, P.M., Kingsolver, J.G., Huey, R.B., 1993. Biotic Interactions and Global Change. Sinauer Associates, Sunderland, MA.

Lactin, D.J., Johnson, R.R., 1998. Environmental, physical, and behavioural determinants of body temperature in grasshipper nymphs (Orthoptera: Acrididae). Can. Entomol. 130, 551–557.

Li, D., Jackson, J.J., 1996. How temperature affects development and reproduction in spiders. J. Thermal Biol. 21 (4), 245–274.

Logan, J.A., Bentz, B.J., 1999. Model analysis of mountain pine beetle seasonality. Environ. Entomol. 28, 924–934.

Logan, J.A., Wollkind, D.J., Hoyt, S.C., Tanigoshi, L.K., 1976. An analytic model for description of temperature dependent rate phenomena in arthropods. Environ. Entomol. 5, 1133–1140.

Logan, J.A., Powell, J.A., 2001. Ghost forests, global warming, and the mountain pine beetle. Am. Entomologist 47 (3), 160–172.

Logan, J.D., 2006. Applied Mathematics, third ed. Wiley-Interscience, New York.

Logan, J.D., Wolesensky, W., Joern, A., 2006. Temperature-dependent phenology and predation in arthropod systems. Ecol. Modelling 196, 471–482.

Logan, J.D., Wolesensky, W., Joern, A., 2007. Insect development under predation risk, variable temperature, and variable food quality. Math. Biosciences and Engineering 4 (1), 47–65.

Logan, J.D., Wolesensky, W. Accounting for temperature in predator functional responses. Natural Resource Modeling, in press.

Mack, J.A.J., Smilowitz, Z., 1982. Using temperature-mediated functional responses models to predict the impact of *Coleomegilla maculata* (DeGreer) adultsand 3rd-instar larvae on green peach aphids. Environ. Entomol. 11, 46–52.

Metz, J.A.J., Diekmann, O., eds 1986. The Dynamics of Physiologically Structured Populations, Springer, Berlin.

Neuman, J.A., 2003. Climate change and cereal aphids: the relative effects of increasing CO_2 and temperature on aphid population dynamics. Global Change Biol. 10, 5–15.

Powell, J.A., Jenkins, J.L., Logan, J.A., Bentz, B.J., 2000. Seasonal temperature alone can synchronize life cycles. Bull. Math. Biol. 62, 977–998.

Quinn, M.A., Kepner, R.L., Walgenbach, D.D., Foster, R.N., Bohls, R.A., Pooler, P.D., Reuter, K.C., Swain, J.L., 1993. Grasshopper stages of development as indicators of nontarget arthropod activity: implications for grasshopper management programs on mixed-grass rangeland. Environ. Entomol. 22, 532–540.

Rochat, J., Gutierrez, A.P., 2001. Weather-mediated regulation of olive scale by two parasitoids. J. Animal Ecology 70, 476–490.

de Roos, A.M., 1997. A gentle introduction to physiologically structured population models. In: Tuljapurkar, S., Caswell, H. (Eds.), Structured-Population Models in Marine, Terrestrial, and Freshwater Systems. Chapman & Hall, New York, pp. 119–204 (Chapter 5).

Shenk, H.J., 1996. Modeling the effect of temperature on growth and persistence of tree species: a critical review of tree population models. Ecol. Modell. 92, 1–32.

Turner, M., 1979. Diet and feeding phenology of the green lynx spider: *P. viridans* (Areneae: oxyopidae). J. Arachnol. 7, 149–154.

Visser, M.E., Holleman, L.J.M., 2001. Warmer springs disrupt the synchrony of oak and winter moth phenology. Proc. R. Soc. B 268, 289–294.

Visser, M.E., Both, C., 2005. Shifts in phenology due to global climate change: the need for a yardstick. Proc. Roy. Soc. B 272, 2561–2569.

Walther, G.-R., Post, E., Convey, P., Menzel, A., Parmesan, C., Beebee, T.J.C., Fromentin, J.-M., Hoegh-Guldberg, O., Bairlein, F., 2002. Ecological responses to recent climate change. Nature 416, 389–395.

Wermelinger, B., Seifert, M., 1999. Temperature dependent reproduction of the spruce bark beetle *Ips yypographus*, and the analysis of the potential population. Ecol. Entomol. 24, 103–110.

Wolesensky, W., Logan, J.D., 2007. An individual, stochastic model of growth incorporating state-dependent risk and random foraging and climate. Math. Biosciences and Engineering 4 (1), 67–84.

Wollkind, D., Logan, J.A., 1978. Temperature-dependent predator-prey mite ecosystem on apple tree foliage. J. Math. Biol. 6, 265–283.

Xia, J.Y., van der Werf, W., Rabbinge, W., 1999. Temperature density of bionomics of Coccinella septempunctata (Coleoptera: Coccinellidae) feeding on Aphis gossyooi (Homoptera: Aphididae) on cotton. Environ. Entomol. 28 (2), 307–314.